1,2-Dioleoyl-3-Trimethylammonium-Propane (DOTAP)-Formulated, Immune-Stimulatory Vascular Endothelial Growth Factor A Small Interfering RNA (siRNA) Increases Antitumoral Efficacy in Murine Orthotopic Hepatocellular Carcinoma with Liver Fibrosis

Miroslaw Kornek,[1] Veronika Lukacs-Kornek,[2] Andreas Limmer,[2] Esther Raskopf,[1] Ursula Becker,[1] Maren Klöckner,[1] Tilman Sauerbruch,[1] and Volker Schmitz[1]

[1]Department of Internal Medicine I, University Hospital Bonn, Germany; [2]Institute of Molecular Medicine and Experimental Immunology (IMMEI), Bonn, Germany

Most experimental therapy studies are performed in mice that bear subcutaneous or orthotopic hepatoma but are otherwise healthy and nonfibrotic. The majority of hepatocellular carcinoma (HCC), however, develops in patients suffering from preexisting liver fibrosis. We investigated the efficacy of a standard experimental therapeutic approach to interrupt the vascular endothelial growth factor (VEGF)/VEGF receptor (VEGFR) cascade via VEGF-A silencing, with or without 1,2-dioleoyl-3-trimethylammonium-propane (DOTAP; cationic lipid) formulation, in HCC mice with preexisting liver fibrosis. The data show that intraperitoneal treatment with naked VEGF-A small interfering RNA (siRNA; 200 μg/kg) was inefficient to treat HCC implanted into fibrotic livers. VEGF-A siRNA containing an immunostimulatory motif in combination with DOTAP formulation significantly reduced hepatic VEGF-A expression and additionally activated the innate and adapted immune system as shown by an increased intrahepatic interferon type 1 response (68-fold increased β-interferon expression). DOTAP-formulated VEGF-A siRNA markedly improved VEGF-A siRNA uptake and enhanced the antitumor response. This study shows for the first time the therapeutic feasibility of using synergistic effects (gene silencing and activation of the immune system) united in one siRNA sequence to reduce HCC growth and metastasis in mice with preexisting liver fibrosis. We expect that these results will help to direct and improve future experimental gene-silencing approaches and establish more efficient antitumoral therapies against HCC.

Online address: http://www.molmed.org
doi: 10.2119/2008-00003.Kornek

INTRODUCTION

In 1978, the World Health Organization defined cirrhosis as "a diffuse process characterized by fibrosis and the conversion of normal liver architecture into structurally abnormal nodules." One of the most common causes of hepatic fibrosis is chronic alcohol abuse; other factors also have the potential to trigger hepatic fibrogenesis (1).

Liver fibrosis is of utmost relevance for hepatocellular carcinogenesis (HCC). Malignant hepatocellular transformation is characterized by a shortened half-life and increased proliferation and regeneration of hepatocytes secondary to ongoing inflammation (2). This leads to accumulation of genomic mutations and instability, alterations that sometimes accumulate in a neoplastic phenotype (3). For that reason, HCC is strongly associated with chronic liver diseases, including chronic hepatitis and cirrhosis. In fact most cases of HCC, approximately 80%, occur in combination with underlying cirrhosis (4,5); <10% are observed in noncirrhotic livers, rarely without hepatitis (6). Notably, once cirrhosis is established there is no proven effective HCC prevention, yet (7). Recently, we showed that hepatic fibrosis relevantly accelerates orthotopic HCC tumor growth and metastasis in fibrotic C3H/He mice (8). Kuriyama *et al.* (9) reported that fibrosis seemed to affect metastasis. However, there is still the need for a robust murine liver fibrosis model to investigate antitumor efficacy.

Angiogenesis plays a major role in a wide range of biological processes, such

Address correspondence and reprint requests to *Volker Schmitz, Medizinische Klinik I, Sigmund-Freud-Str. 25, 53105 Bonn, Germany. Phone: + 49/228-28716469; Fax: + 49/228-28714698; E-mail: volker.schmitz@ukb.uni-bonn.de; or Miroslaw Kornek, Medizinische Klinik I, Sigmund-Freud-Str. 25, 53105 Bonn, Germany. Phone: + 49/228-28711033; E-mail: miroslawkornek@web.de.*
Submitted January 12, 2008; Accepted for publication March 25, 2008; Epub (www.molmed.org) ahead of print March 26, 2008.

as wound healing, organ regeneration, and the female reproduction cycle. Under normal conditions, angiogenesis otherwise does not occur in an adult organism but is needed for further tumor growth. Vascular endothelial growth factor (VEGF) is a major player in tumor angiogenesis, and the VEGF/VEGF receptor (VEGFR) pathway is a major focus of interest in basic cancer research (10). Several studies have used gene silencing targeted against VEGF-A mRNA in distinct tumor models (11–14).

There are no data on functional VEGF-A knockdown in HCC with preexisting hepatic fibrosis. Here, we applied 1,2-dioleoyl-3-trimethylammonium-propane (DOTAP)-formulated small interfering RNA (siRNA) targeted against VEGF-A to control HCC in mice with preexisting hepatic fibrosis.

MATERIALS AND METHODS

Animals and Cell Lines

C3H/He female mice (age matched) were obtained from Charles River (Sulzfeld, Germany) and housed under SPF conditions in the central animal facility of the University Hospital Bonn. Animal procedures were performed in accordance with approved protocols of the responsible local governmental administration and followed recommendations for proper care and use of laboratory animals.

Hepa129 cells (hepatoma 129 originating from C3H/He mice, obtained from NCI-Frederick Cancer Research and Development Center [DCT Tumor Repository; Frederick, MD, USA]) were maintained in RPMI 1640 (Invitrogen, Karlsruhe, Germany) supplemented with 10% fetal calf serum (FCS) (Invitrogen), 200 mM glutamine, and penicillin/streptomycin.

Administration of Thioacetamide and EtOH

Before tumor cell implantation, induction of fibrosis was studied in female C3H/He mice using i.p. injections of thioacetamide (TAA) (Sigma-Aldrich, Taufkirchen, Germany; 0.15 mg/g body weight) three times per wk for up to 24 wks in combination with alcohol feeding in sweetened drinking water (10% vol/vol) according to a published protocol (8,15,16).

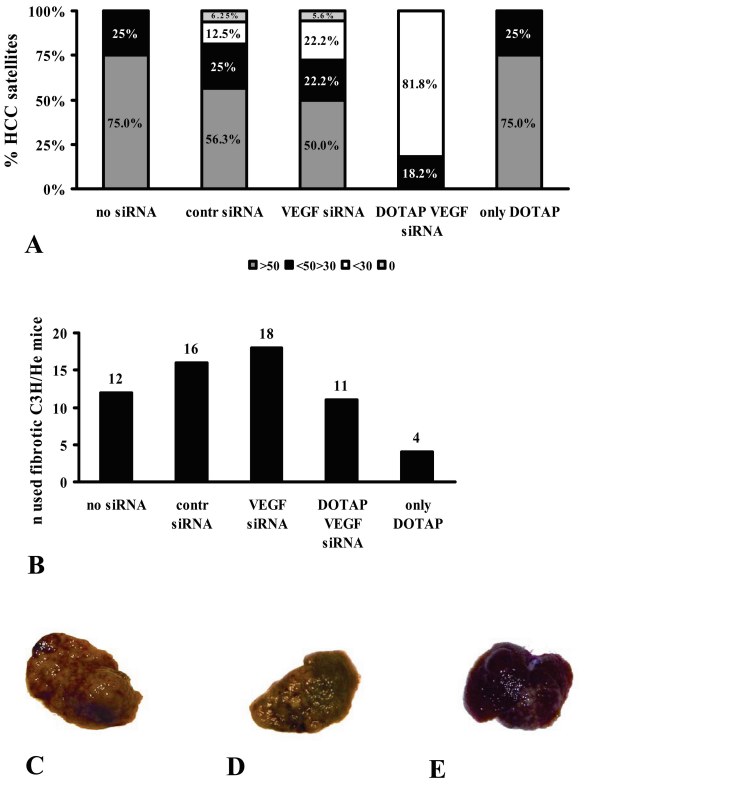

Figure 1. (A) Antitumoral effects of naked VEGF-A siRNA silencing with or without DOTAP formulation. DOTAP VEGF-A siRNA significantly reduced surface HCC satellites in fibrotic mice 11 days after Hepa129 HCC tumor cell implantation. Treated mice were divided into four groups: >50, <50 and >30, <30, and no surface satellites. These data were generated by two independent experiments. (B) Numbers of mice in each group. (C, D, and E) Representative livers. (C), >50; (D), <50 and >30; (E), <30.

Tumor Cell Implantation

Fibrotic mice were anesthetized with ketamine (Pharmacia GmbH, Karlsruhe, Germany) 0.1 mg/g body weight and xylazine 2% (Rompun; aniMedica GmbH, Senden-Boesensell, Germany) 0.01 mg/g body weight. Laparotomy for syngenic tumor cell implantation was performed as described elsewhere. (17) Briefly, 64 fibrotic mice were laparotomized and orthotopic tumors were established by subcapsular intrahepatic injection of 1.25×10^5 hepatoma cells (Hepa129) suspended in 50 µL RPMI into the left liver lobe. Postinjection bleeding and tumor cell escape were avoided by local compression. Laparotomy was closed in two layers by continuous suture with absorbable material. To allow comparative statistical analysis, HCC satellites visible at the liver surface were counted and mice were divided into four subgroups (two independent experiments; mice numbers of each cohort are given in Figure 1B) depending on the number of satellites: a subgroup with >50, <50 and >30, <30, and no visible surface HCC satellites. Additionally, blood samples were taken from all four cohorts for analysis at d 11 postimplantation. TAA injections were continued after tumor cell implantation.

To minimize postoperational mortality, TAA administration was paused for up to 7 d after tumor cell implantation.

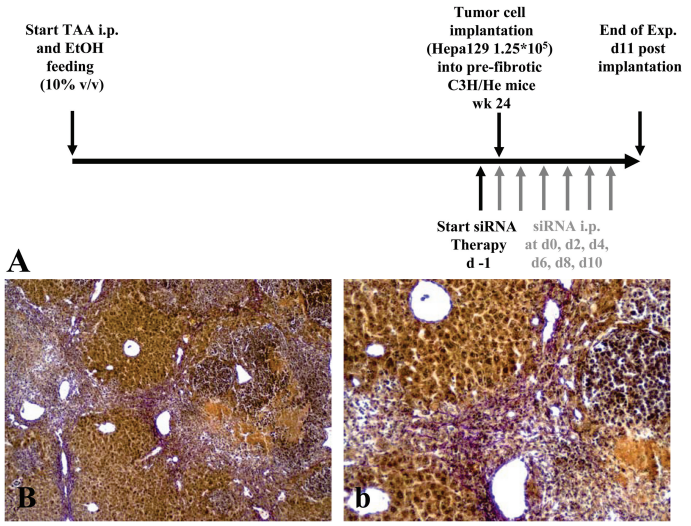

Figure 2. (A) Overview of the experimental setting. Fibrosis was induced by the combination of TAA i.p. injections three times per wk and with an additional continuous supplement of EtOH (10% vol/vol) in the drinking water. At wk 24, Hepa129 HCC tumor cells were implanted into fibrotic mice livers and treated with VEGF-A siRNA with different formulations. (B and b) Representative paraffin sections of fibrotic liver samples with intrahepatic HCC satellites 11 d after implantation. Fibrosis was staged according to the score system proposed by Ishak *et al.* (16). Original magnification 40× (B), 100× (b).

At d 7 and 9, all mice received TAA i.p. again. EtOH feeding via drinking water was maintained.

siRNA

siRNA used in this study were purchased from Dharmacon/Perbio Science Deutschland (Bonn, Germany) and received as desalted, pre-annealed duplexes in standard purified batches. One siRNA batch was fluorescein labeled for evaluation of the transfection efficiency. The sense strands sequences were as follows: VEGF, 5´-AUGUGAAUGC AGACCAAAG AA-dTdT; CONTRL, 5´-GAUAGCAAUGACGAAU GCGUA-dTdT, according to a publication by Filleur *et al.* (18).

DOTAP was purchased from Roth (Karlsruhe, Germany). The DOTAP siRNA complex was formulated according to the manufacturer's protocol and adapted to the *in vivo* application. Fibrotic mice received 200 µg siRNA/kg body weight (5 µg siRNA for a 27-g mouse) according to published studies (18–20). The DOTAP siRNA ratio was 2:1 (vol/wt). Therefore, 5 µg siRNA were incubated with 10 µL DOTAP for 20 min at room temperature and diluted in NaCl (0.9%) buffer for i.p. injections. siRNA was applied i.p. as described (21). siRNA with or without DOTAP formulation was injected at day –1, day 0 (HCC implantation), and every second d until d 10 (Figure 2A).

Histology

For van Gieson staining, 4% formaldehyde-fixed liver samples were paraffin embedded, and 5-µm sections were stained according to a standard protocol. Fibrosis was assessed according to the fibrosis scoring system proposed by Ishak *et al.* (22) (no fibrosis F0, cirrhosis F6).

To determine cell proliferation, cryopreserved liver sample sections were immunostained with rabbit antimouse Ki-67 (1:25; Dako, Hamburg, Germany) and incubated with a biotinylated antirabbit swine IgG secondary antibody (Dako) and streptavidine peroxidase. Enzymatic activity was developed using 3-amino-9-ethylcarbazole (AEC; Dako) as substrate, and sections were counterstained with Mayer hematoxylin. For Ki-67 immunofluorescence staining, cryopreserved liver sample sections from FL-siRNA-treated (±DOTAP) fibrotic HCC implanted mice were immunostained with rat antimouse Ki-67 (1:25; Dako) and incubated with Alexa Fluor 546 goat antirat secondary antibody (Molecular Probes, Leiden, The Nederlands).

RNA, cDNA Preparation, and Semiquantitative Real-Time PCR (Liquid Chromatography)

Murine RNA was isolated from tumor tissue samples using the HighPure RNA Isolation Tissue Kit (Roche Diagnostics, Mannheim, Germany) according to the manufacturer's protocol. RNA concentrations were determined and 10 µL RNA was used in the reverse-transcription reaction with random primers (Transkriptor cDNA Synthesis Kit; Roche Diagnostics). Transcript levels of VEGF-A, interferon (IFN)-β, and hypoxia-inducible factor (HIF)-1α were determined in relation to 18sRNA mRNA levels by semiquantitative real-time PCR (LightCycler; Roche Diagnostics). Primers were obtained from Invitrogen GmbH and probes from Roche Diagnostics. Sequences are given in Table 1.

Statistical Analysis

All data are given as arithmetic means with SD. Differences between values of independent experimental groups were analyzed for statistical significance by Mann-Whitney *U* test. An error level $P < 0.05$ indicates significance.

RESULTS

Histological and Immunohistological Assessment of Fibrosis

To verify liver fibrosis induction, van Gieson staining was performed 11 d after tumor cell implantation in paraffin sections from fibrotic mice treated for 24 wks with TAA i.p. and EtOH (Figure 2A). Similar to our previous publication (15), livers of TAA- and EtOH-treated mice showed fibrotic septa with predominant

Table 1. Specific primer oligonucleotides and oligonucleotide probes for PCR.

Target gene	5′-primer	Probe	3′-primer
18sRNA	AAA TCA GTT ATG GTT CCT TTG GTC	TCC TCT CC	GCT CTA GAA TTA CCA CAG TTA TCC AA
VEGF-A	GCA GCT TGA GTT AAA CGA ACG	CCA GGC TG	GGT TCC CGA AAC CCT GAG
IFN-β	ACA GCC TTT GCC TCA TCT TG	CAG CCT CG	TGG AGG ATC CAC CTG TTG TT
TNF-α	CTG TAG CCC ACG TCG TAG C	TGG AGG AG	TTG AGA TCC ATG CCG TTG
HIF-1α	CAT GAT GGC TCC CTT TTT CA	CAG CAG GA	GTC ACC TGG TTG CTG CAA TA

porto-porto bridging (Figure 2B and b). Additionally, hepatic regeneration nodules could be detected in several mice. When applying the Ishak scoring system (22), fibrosis was graded F4/5 (maximum F6).

Influence on Hepa129 Tumor Growth after Treatment with VEGF-A siRNA

Syngenic Hepa129 tumor cell implantation resulted in numerous HCC satellites in these fibrotic mice. In untreated mice, practically the complete left liver lobe was infiltrated by innumerable HCC satellites. No primary tumor nodule was distinguishable in these severely tumor-infiltrated livers. Eleven d after tumor cell implantation, HCC satellites were counted and four subgroups were selected depending on the satellite count (Figure 1A): >50 (Figure 1C), <50 and >30 (Figure 1D), <30 (Figure 1E), and no visible surface lesions.

In untreated control mice, 75% of the mice had >50 satellites and only 25% had <50 and >30 surface satellites. In the siRNA control group, some antitumor effects of scrambled control siRNA were observed: 25% of these mice had <50 and >30, 12.5% <30, and 6.25% no surface satellites at all. The distribution pattern between control siRNA and naked VEGF-A siRNA differed only slightly: 50% of the naked VEGF-A siRNA treated mice did not respond, about 22% had <50 and >30 surface satellites, 22% had <30, and 5.7% had no observable surface satellites.

In contrast to the results of treatment with naked VEGF-A siRNA, the DOTAP VEGF-A siRNA complex increased the antitumoral treatment efficacy in orthotopic hepatomas developing in liver fibrosis. The percentage of mice with <30 surface satellites increased by almost fourfold, from average 22% in the naked VEGF-A siRNA group to 82% in the corresponding DOTAP-formulated VEGF-A siRNA treatment group. Only 18% of mice treated with DOTAP VEGF-A siRNA had <50 and >30 surface satellites, and none had >50 surface satellites.

In line with previous results that DOTAP alone did not affect or activate the innate or adaptive immune system, the tumor burden of mice that had solely been injected with DOTAP fully resembled that of the control group. These data stem from two independent experiments; the detailed group sizes are given in Figure 1B.

Ki-67 Staining for Determination of Intratumoral Proliferating Cells 11 Days after siRNA Treatment Initiation

Proliferation of tumor satellites in fibrotic mice was demonstrated by Ki-67 staining (Figure 3). Extension of HCC satellite area was measured before Ki-67 cell count by microscope software. Ki-67 cells were quantified in size-matched satellites in samples from VEGF-A siRNA–treated mice with or without DOTAP formulation. Ki-67 proliferation did not differ between control siRNA and naked VEGF-A siRNA without DOTAP, whereas DOTAP VEGF-A siRNA

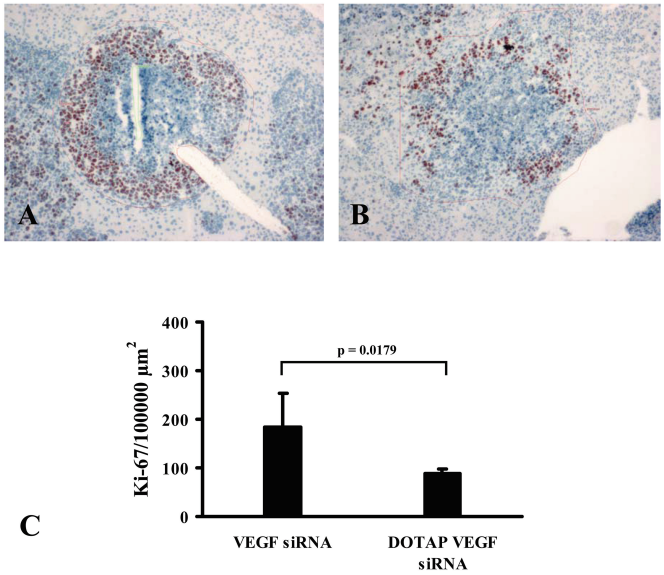

Figure 3. (A and B) Representative proliferation marker (Ki-67) staining for determination of intratumoral proliferating cells 11 d after treatment initiation. Ki-67 staining showed significant differences between naked VEGF-A siRNA and DOTAP VEGF-A siRNA mice (A, VEGF-A siRNA; B, DOTAP VEGF-A siRNA, original magnification 64×). (C) Ki-67 statistical analysis for Ki-67–positive cells counted in HCC satellites. Satellite areas were measured before count with analyzing microscope software, and only Ki-67–positive cells were counted in size-matched satellites. Ki-67 count was significantly higher in HCC satellites obtained from mice that had been treated with naked VEGF-A siRNA compared with DOTAP VEGF-A siRNA.

markedly reduced Ki-67–positive cells in the HCC satellites (Figure 3A and B). Statistical analysis showed a significantly higher number of Ki-67–positive cells (2.1-fold) in naked VEGF-A siRNA compared with DOTAP VEGF-A siRNA (Figure 3C).

DOTAP FL-VEGF siRNA Detection

To investigate the uptake of siRNA, naked or complexed with DOTAP, fluorescein-labeled siRNA was injected according to our standard treatment protocol and analyzed for hepatic distribution (Figure 4A and B). Considering elevated intratumoral VEGF-A expression and diminished hepatic VEGF expression, we expected that dye-labeled siRNA would be taken up not by the tumor but by hepatic tissue. Representative fluorescence images showed that mainly Ki-67–negative, presumably nontumoral cells distant to HCC satellites had taken up labeled siRNA independent of the siRNA formulation. DOTAP formulation uptake clearly enhanced the labeled siRNA uptake even at the tumor edge (Figure 4A and B).

DOTAP VEGF-A siRNA Effect on Hepatic VEGF-A Expression

According to the uptake results, semiquantitative PCR results carried out against hepatic VEGF-A confirmed that the DOTAP VEGF-A siRNA formulation decreased VEGF-A transcription by a factor of 2.6 (62%) in peritumoral hepatic tissue compared with animals that did not receive any siRNA treatment (Figure 4A). Compared with mice treated with scrambled control siRNA, DOTAP VEGF-A siRNA significantly reduced hepatic VEGF-A by a factor of 1.7 (41%). When naked VEGF-A siRNA and DOTAP VEGF-A siRNA treatments were compared, intrahepatic VEGF-A silencing was considerably improved by a factor of 3 in favor of DOTAP siRNA VEGF-A. Again, no significant differences were measurable between the cohort treated with DOTAP alone and untreated controls.

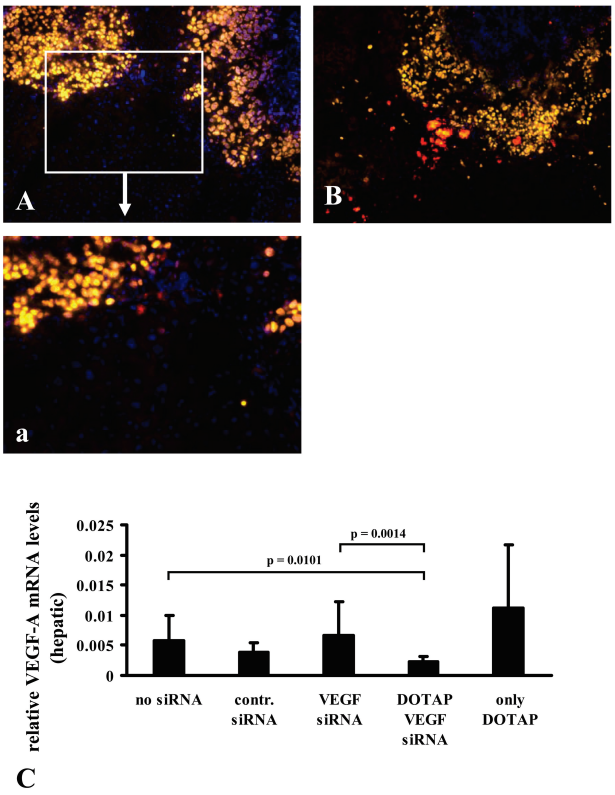

Figure 4. (A, a, and B) Representative images from mice treated either with fluorescein-labeled naked siRNA without DOTAP formulation (A and a) or with DOTAP fluorescein-labeled siRNA (B). Original magnification 100× (A/B), 200× (a). (C) Effect of DOTAP-formulated naked VEGF-A siRNA on hepatic VEGF expression. Gene silencing was significantly increased by the use of DOTAP VEGF-A siRNA compared with naked VEGF-A siRNA ($P = 0.0014$).

DOTAP VEGF-A siRNA Effect on Intratumoral VEGF-A and HIF-1α Expression

At first sight, it was somewhat unexpected that intratumoral VEGF-A transcription was not reduced with any siRNA treatment, naked VEGF-A siRNA or DOTAP VEGF-A siRNA (Figure 5A). Instead, the highest intratumoral VEGF-A transcription values (14-fold increased) were observed in DOTAP VEGF-A siRNA compared with scrambled control siRNA. Treatment with DOTAP alone elevated intratumoral VEGF. Naked VEGF-A siRNA resulted in a minor 1.3-fold intratumoral transcription increment.

Increased intratumoral VEGF-A expression was paralleled by raised intratumoral HIF-1α transcription (7.4-fold) in DOTAP VEGF siRNA–treated mice compared with untreated mice (Figure 5B). Naked VEGF-A siRNA also slightly augmented (2.7-fold) HIF-1α expression. Again, treatment with DOTAP alone did not affect intratumoral HIF-1α levels compared with untreated controls.

DOTAP VEGF-A siRNA Effect on Hepatic IFN-β Expression

To investigate the activation status of the immune system, IFN-β was selected as a member of the interferon type 1 family. We investigated the hepatic transcription of IFN-β in the tumor surrounding fibrotic liver tissue at the end of the experiment (d 11 after tumor cell implantation, the last time point of the last siRNA application) (Figure 6A). As expected from published data (23), no significant immune system activation was seen in animals treated with naked siRNA lacking DOTAP. In contrast, the injection of a

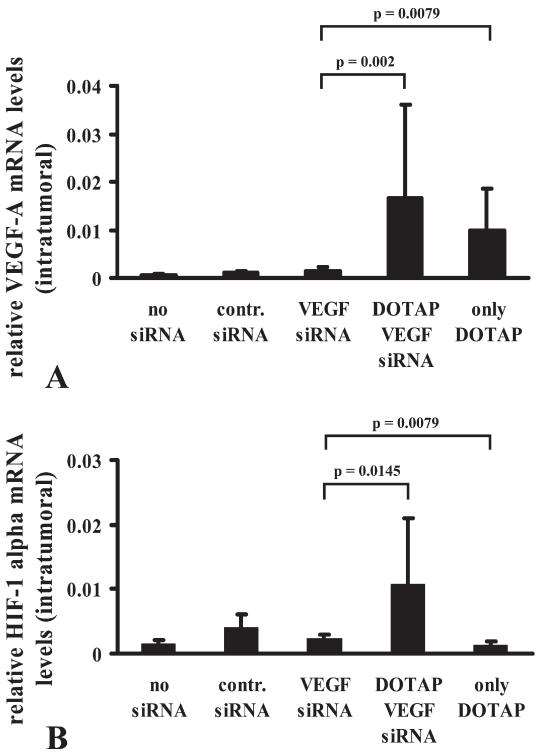

Figure 5. LightCycler VEGF-A and HIF-1α semiquantitative data showed marked intratumoral VEGF-A (A, $P = 0.002$) and intratumoral HIF-1α (B, $P = 0.0145$) upregulation due to DOTAP VEGF-A siRNA treatment.

DOTAP-formulated siRNA sequence that contains an immunostimulatory motif (23) (Figure 6A) induced an IFN type 1 response (23–25). Consistent with these publications, DOTAP VEGF-A siRNA led to a significant 68-fold increased IFN-β response compared with naked VEGF siRNA; treatment with DOTAP alone did not induce an IFN-β response.

DOTAP VEGF-A siRNA Effect on Hepatic Tumor Necrosis Factor-α Expression

DOTAP VEGF-A siRNA did not elevate tumor necrosis factor (TNF)-α expression but rather decreased it significantly, by 66% compared with naked VEGF-A siRNA treatment (Figure 6C). Interestingly, treatment with DOTAP alone resulted in TNF-α reduction by 92% compared with naked VEGF-A siRNA. In fact TNF-α stimulates a Th-1–– mediated immune response and might therefore add, if elevated, to antitumoral effect of a DOTAP-complexed VEGF-A siRNA treatment. Because TNF-α upregulation was monitored in neither DOTAP- nor DOTAP siRNA–injected mice, stimulation of the Th-1–mediated immune response by TNF-α can be ruled out, as suggested by others (26).

DISCUSSION

Because HCC predominantly develops in damaged fibrotic liver tissue, it is desirable to combine hepatoma growth and chronic liver damage to imitate most closely the disease course of HCC in humans. This study was designed to elucidate the antitumor efficacy of an anti–VEGF-A HCC treatment in liver fibrosis. For this purpose, liver fibrosis was induced by a combination of TAA i.p. and EtOH. Once liver fibrosis was established, hepatomas were induced by tumor cell implantation. Subsequently, a functional VEGF-A knockdown applying different formulations of VEGF-A siRNA was used to interrupt the VEGF/VEGFR cascade in this model. Tumor burden and protein expression of related genes, namely VEGF-A and HIF-1α, were quantified. In this setting, the antitumor response could partly be attributed to immune-stimulating features of the siRNA sequence and partly to gene silencing of the VEGF-A target gene.

Several studies have been carried out to target the VEGF/VEGF receptor pathway via siRNA to treat tumors of different origin, like retinoblastoma, prostate carcinoma, colon adenocarcinoma, colon cancer, and glioblastoma *in vitro* and *in vivo* (12,13,27,28). Considering the role of VEGF in HCC, anti-VEGF therapies are of particular interest for this tumor entity. Usually, experimental antitumor strategies are tested in subcutaneous, but rarely in orthotopic, hepatoma models (29,30). Previously, the Hepa129 hepatoma cell line has been demonstrated to be suitable for orthotopic tumor growth and also for therapeutic intervention studies (29,31). Furthermore, our previous data demonstrated that liver fibrosis had a strong impact on orthotopic HCC growth. It appeared that preexisting fibrosis modulated Hepa129 tumor growth in such a way that tumor growth was accelerated by forming innumerous tumor satellites (8,16).

In this study, liver damage by TAA i.p. and EtOH administration resulted in F4/5 fibrosis as demonstrated by van Gieson collagen staining. Consonant with our former findings, orthotopic HCC growth severely infiltrated liver tissue in the case of preexisting fibrosis. In spite of VEGF upregulation in this model, treatment with naked VEGF-A siRNA did not relevantly inhibit tumor load. This finding was somewhat unexpected, because previous studies including our own using the same naked VEGF-A siRNA sequence achieved significant antitumoral effects in a prostate cancer s.c. xenograft model and also in Hep129 hepatomas in nonfibrotic mice (19,32). In the former models, tumors generally developed as single nodules that were successfully treated with

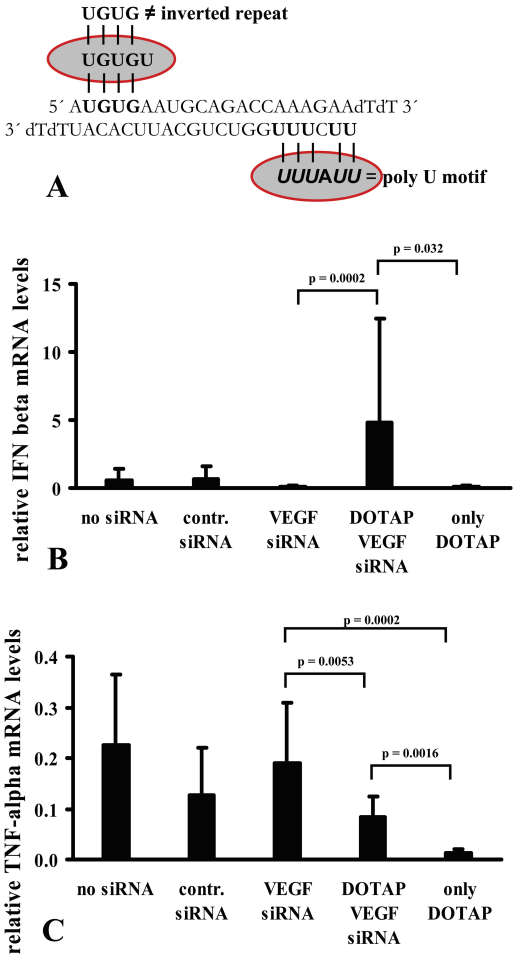

Figure 6. (A) Naked VEGF-A siRNA sequence. Highlighted: immunostimulatory motifs as proposed by Judge *et al.* (23). The naked VEGF-A siRNA sequence contains a poly U motif on the siRNA antisense strain that is supposed to activate the immune system if formulated with DOTAP. (B and C) DOTAP VEGF-A siRNA effect on intrahepatic IFN-β (B) and TNF-α (C) expression after systemic i.p. administration of DOTAP-formulated VEGF-A siRNA and naked VEGF-A siRNA, respectively.

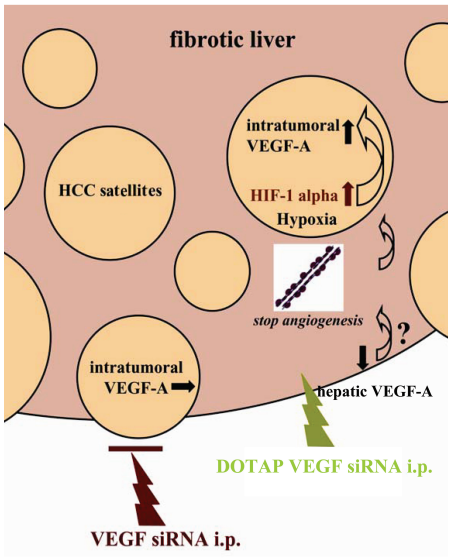

Figure 7. A simplified overview elucidating our hypothesis: siRNA uptake is improved by efficacy due to formulation with DOTAP, whereas naked VEGF-A siRNA treatment results in low uptake, inducing only limited gene knockdown and low antitumoral efficacy.

the naked VEGF-A siRNA preparation. In contrast to those works, tumor growth was diffuse and infiltrative in the recent fibrotic HCC model. Thus, loss of antitumor efficacy may be attributed to irrelevance of VEGF-A in this model or to decreased siRNA uptake efficiency *in vivo* in liver fibrosis. Roberts *et al.* (33) blocked VEGFR3 with a neutralizing antibody, resulting in decreased metastasis *in vivo*. Here, we intended to overcome antitumor inefficacy of naked VEGF-A siRNA by DOTAP siRNA formulation. Indeed, labeled naked siRNA uptake was strongly improved when formulated with DOTAP, whereas intrahepatic and intratumoral fluorescence signals were rarely detectable in mice injected with naked siRNA. Enhanced uptake was well reflected in decreased hepatic expression of the target gene VEGF-A. It has been shown by others that naked siRNA modifications such as PEG formulation increase VEGF-A siRNA stability and protect against enzymatic degradation (11). Furthermore Liu *et al.* (34) reported that injection of lipoplexes through the portal vein after partial hepatectomy induced higher reporter gene expression (luciferase) in the liver than naked DNA injection. This earlier study already showed that the DOTAP formulation of DNA boosted its uptake and enhanced transfection efficiency.

Judge *et al.* (23) reported that DOTAP and poly U–rich siRNA complexes activate the innate and adapted immune system via IFN type 1 upregulation. The VEGF-A siRNA sequence employed in our study also contains a poly U–rich motif, which may trigger activation of the innate and adapted immune system via IFN type 1 upregulation as suggested. So far, three different immune-stimulatory siRNA motifs have been described; none of these were capable of inducing an IFN type 1 response without DOTAP (23,24). A current review suggested that the merging of gene-silencing and immune-stimulation siRNA in one siRNA molecule may provide "two edges of one sword for effective treatment of cancer" (25). Consonant with the former finding, naked VEGF-A siRNA containing an immune-stimulatory motif did not induce IFN type 1 increase,

confirming published *in vitro* and *in vivo* data (24,35,36). In contrast, hepatic IFN type 1 levels increased 68-fold in DOTAP VEGF-A siRNA–treated mice. IFNs might attribute to antitumoral efficacy in this setting by modulation of proliferation, differentiation, and the immune system (37). It has been reported that the systemic administration or gene delivery of IFNs exerted a therapeutic effect in some experimental models (38–40). Interestingly, it has been shown that high-dose and long-term therapy with IFNs inhibited experimental HCC development and that IFN-β prevented recurrence of HCC in humans with chronic hepatitis C virus infection (41–43). Considering IFN expression levels in our study, IFNs (IFN type I) might add up to overall antitumor efficacy by anti-angiogenic or antiproliferative effects in this HCC model.

TNF-α is a well-known pro-inflammatory cytokine related to the Th-1 innate immune response. Together with IFN-β, TNF-α might be affected by siRNA and carry additional antitumor effects. However, Khazanov *et al.* (26) demonstrated that DNA-based lipoplexes (DOTAP) resulted in low levels of TNF-α, along with others. They concluded that the observed antitumoral effect cannot be ascribed to Th-1 inflammation, but rather to a direct cytotoxic effect on the tumor cells. Our DOTAP-only results ruled out the latter hypothesis, because we did not observe any tumor load differences between the untreated and the DOTAP-only cohorts.

In spite of DOTAP formulation, the tumor itself was practically barred out by siRNA uptake *in vivo*, although uptake was boosted in surrounding nontumoral liver tissue. This observation probably explains why in spite of decreased VEGF-A levels in peritumoral hepatic tissue, intratumoral VEGF-A was not reduced; intratumoral levels were even significantly increased (14-fold). These results are in line with intratumoral HIF-1α data showing a significant (7.4-fold) increment only in the DOTAP VEGF-A siRNA–treated mice (44–46). Because HIF-1α upregulation can be assumed to indicate an intratumoral oxygen deficiency (47), reduced tumor cell proliferation can most plausibly be attributed to intratumoral low oxygen tension in this model. This finding is well reflected by our Ki-67 results (Figure 7).

In earlier studies, we demonstrated that tumor-bearing nonfibrotic mice that were systemically treated with AdsFlk-1 showed a strong increase of circulating VEGF, whereas VEGF remained at background levels in controls. Furthermore, VEGF determination in liver tissue homogenates showed a 16.5-fold increase in AdsFlk-1–treated animals compared with AdLacZ controls (30). Additionally, Bocci *et al.* (48) suggested that detection of elevated VEGF values even presents a suitable biochemical surrogate marker for antitumor response to a successful antitumoral therapy, although we did not confirm this finding in AdsFlk-1–treated colorectal cancer (30).

In summary, naked VEGF-A siRNA was ineffective to control tumor load in liver fibrosis in this study, whereas DOTAP VEGF-A siRNA reestablished antitumor efficacy partially because of improving intratumoral siRNA uptake. Our data imply that immune-stimulatory siRNA motifs can work in concert with target-specific gene silencing. Thus, the purposeful design of a DOTAP-formulated siRNA sequence targeting a specific tumor relevant gene and simultaneously inducing an immune-stimulatory effect can be helpful to treat experimental HCC.

ACKNOWLEDGMENTS

This work was partly supported by a Deutsche Krebshilfe and a DFG grant to V.S. No conflicts of interest exist.

We thank Prof. P.A. Knolle, head of the Institute of Molecular Medicine and Experimental Immunology (IMMEI, Bonn, Germany) for continuous support of the project. Additionally we thank our practicum-student Bettina Schroll for her assistance during the tumor implantation surgery.

REFERENCES

1. Anthony PP *et al.* (1978) The morphology of cirrhosis: recommendations on definition, nomenclature, and classification by a working group sponsored by the World Health Organization. *J. Clin. Pathol.* 31:395–414.
2. Guo JT *et al.* (2000) Apoptosis and regeneration of hepatocytes during recovery from transient hepadnavirus infections. *J. Virol.* 74:1495–505.
3. Liang TJ, Heller T. (2004) Pathogenesis of hepatitis C-associated hepatocellular carcinoma. *Gastroenterology* 127: S62–71.
4. Johnson RC. (1997) Hepatocellular carcinoma. *Hepatogastroenterology* 44:307–12.
5. Llovet JM, Burroughs A, Bruix J. (2003) Hepatocellular carcinoma. *Lancet* 362:1907–17.
6. Bluteau O *et al.* (2002) Bi-allelic inactivation of TCF1 in hepatic adenomas. *Nat. Genet.* 32:312–5.
7. Camma C, Giunta M, Andreone P, Craxi A. (2001) Interferon and prevention of hepatocellular carcinoma in viral cirrhosis: an evidence-based approach. *J. Hepatol.* 34:593–602.
8. Kornek M *et al.* (2008) Accelerated orthotopic hepatocellular carcinomas growth is linked to increased expression of pro-angiogenic and prometastatic factors in murine liver fibrosis. *Liver Int.* 28:509–18.
9. Kuriyama S *et al.* (1999) Hepatocellular carcinoma in an orthotopic mouse model metastasizes intrahepatically in cirrhotic but not in normal liver. *Int. J. Cancer* 80:471–6.
10. Ferrara N, Kerbel RS. (2005) Angiogenesis as a therapeutic target. *Nature* 438:967–74.
11. Kim SH *et al.* (2006) PEG conjugated VEGF siRNA for anti-angiogenic gene therapy. *J. Control. Release* 116:123–9.
12. Mulkeen AL *et al.* (2006) Short interfering RNA-mediated gene silencing of vascular endothelial growth factor: effects on cellular proliferation in colon cancer cells. *Arch. Surg.* 141:367–74.
13. Jia RB *et al.* (2007) VEGF-targeted RNA interference suppresses angiogenesis and tumor growth of retinoblastoma. *Ophthalmic Res.* 39:108–15.
14. Shen HL *et al.* (2007) Vector-based RNAi approach to isoform-specific downregulation of vascular endothelial growth factor (VEGF)165 expression in human leukemia cells. *Leuk. Res.* 31:515–21.
15. Kornek M *et al.* (2006) Combination of systemic thioacetamide (TAA) injections and ethanol feeding accelerates hepatic fibrosis in C3H/He mice and is associated with intrahepatic up regulation of MMP-2, VEGF and ICAM-1. *J. Hepatol.* 45: 370–6.
16. Kornek M *et al.* (2007) Experimental orthotopic HCC growth is accelerated in hepatic fibrosis. *J. Hepatol.* 46:S82–3.
17. Kornek M, Raskopf E, Tolba R, Becker U, Klöckner M, Sauerbruch T, Schmitz V. (2008) Accelerated orthotopic hepatocellular carcinomas growth is linked to increased expression of pro-angiogenic and prometastatic factors in murine liver fibrosis. *Liver Int*. 28(4):509-18.

18. Filleur S *et al.* (2003) SiRNA-mediated inhibition of vascular endothelial growth factor severely limits tumor resistance to antiangiogenic thrombospondin-1 and slows tumor vascularization and growth. *Cancer Res.* 63:3919–22.
19. Takei Y *et al.* (2004) A small interfering RNA targeting vascular endothelial growth factor as cancer therapeutics. *Cancer Res.* 64:3365–70.
20. Verma UN *et al.* (2003) Small interfering RNAs directed against beta-catenin inhibit the *in vitro* and *in vivo* growth of colon cancer cells. *Clin. Cancer Res.* 9:1291–300.
21. Aigner A. (2006) Delivery systems for the direct application of siRNAs to Induce RNA interference (RNAi) *in vivo*. *J. Biomed. Biotechnol.* 2006: 71659.
22. Ishak K *et al.* (1995) Histological grading and staging of chronic hepatitis. *J. Hepatol.* 22:696–9.
23. Judge AD *et al.* (2005) Sequence-dependent stimulation of the mammalian innate immune response by synthetic siRNA. *Nat. Biotechnol.* 23: 457–62.
24. Hornung V *et al.* (2005) Sequence-specific potent induction of IFN-alpha by short interfering RNA in plasmacytoid dendritic cells through TLR7. *Nat. Med.* 11:263–70.
25. Schlee M, Hornung V, Hartmann G. (2006) siRNA and isRNA: two edges of one sword. *Mol. Ther.* 14:463–70.
26. Khazanov E, Simberg D, Barenholz Y. (2006) Lipoplexes prepared from cationic liposomes and mammalian DNA induce CpG-independent, direct cytotoxic effects in cell cultures and in mice. *J. Gene Med.* 8:998–1007.
27. Kim WJ *et al.* (2006) Cholesteryl oligoarginine delivering vascular endothelial growth factor siRNA effectively inhibits tumor growth in colon adeno't takcarcinoma. *Mol. Ther.* 14:343–50.
28. Niola F *et al.* (2006) A plasmid-encoded VEGF siRNA reduces glioblastoma angiogenesis and its combination with interleukin-4 blocks tumor growth in a xenograft mouse model. *Cancer Biol. Ther.* 5:174–9.
29. Raskopf E *et al.* (2005) Effective angiostatic treatment in a murine metastatic and orthotopic hepatoma model. *Hepatology* 41:1233–40.
30. Schmitz V *et al.* (2006) Increased VEGF levels induced by anti-VEGF treatment are independent of tumor burden in colorectal carcinomas in mice. *Gene Ther.* 13:1198–205.
31. Schmitz V *et al.* (2004) Establishment of an orthotopic tumour model for hepatocellular carcinoma and non-invasive *in vivo* tumour imaging by high resolution ultrasound in mice. *J. Hepatol.* 40:787–91.
32. Raskopf E *et al.* (2007) Posttranscriptional VEGF inhibition reduces tumor growth in an experimental murine HCC model. *J. Hepatol.* 46:S151.
33. Roberts N *et al.* (2006) Inhibition of VEGFR-3 activation with the antagonistic antibody more potently suppresses lymph node and distant metastases than inactivation of VEGFR-2. *Cancer Res.* 66:2650–7.
34. Liu L *et al.* (2003) Poly(cationic lipid)-mediated *in vivo* gene delivery to mouse liver. *Gene Ther.* 10:180–7.
35. Hamm S *et al.* (2007) Immunostimulatory RNA is a potent inducer of antigen-specific cytotoxic and humoral immune response *in vivo*. *Int. Immunol.* 19:297–304.
36. Meier A *et al.* (2007) MyD88-dependent immune activation mediated by human immunodeficiency virus type 1-encoded Toll-like receptor ligands. *J. Virol.* 81:8180–91.
37. Hertzog PJ, Hwang SY, Kola I. (1994) Role of interferons in the regulation of cell proliferation, differentiation, and development. *Mol. Reprod. Dev.* 39:226–32.
38. Hong YK *et al.* (2000) Efficient inhibition of *in vivo* human malignant glioma growth and angiogenesis by interferon-beta treatment at early stage of tumor development. *Clin. Cancer Res.* 6:3354–60.
39. Izawa JI *et al.* (2002) Inhibition of tumorigenicity and metastasis of human bladder cancer growing in athymic mice by interferon-beta gene therapy results partially from various antiangiogenic effects including endothelial cell apoptosis. *Clin Cancer Res.* 8:1258–70.
40. Cao G *et al.* (2001) Adenovirus-mediated interferon-beta gene therapy suppresses growth and metastasis of human prostate cancer in nude mice. *Cancer Gene Ther.* 8:497–505.
41. Wang L *et al.* (2000) High-dose and long-term therapy with interferon-alfa inhibits tumor growth and recurrence in nude mice bearing human hepatocellular carcinoma xenografts with high metastatic potential. *Hepatology* 32:43–8.
42. Ikeda K *et al.* (2000) Interferon beta prevents recurrence of hepatocellular carcinoma after complete resection or ablation of the primary tumor-A prospective randomized study of hepatitis C virus-related liver cancer. *Hepatology* 32:228–32.
43. Ogasawara S *et al.* (2007) Growth inhibitory effects of IFN-beta on human liver cancer cells *in vitro* and *in vivo*. *J. Interferon Cytokine Res.* 27: 507–16.
44. Shweiki D, Itin A, Soffer D, Keshet E. (1992) Vascular endothelial growth factor induced by hypoxia may mediate hypoxia-initiated angiogenesis. *Nature* 359:843–5.
45. Forsythe JA *et al.* (1996) Activation of vascular endothelial growth factor gene transcription by hypoxia-inducible factor 1. *Mol. Cell. Biol.* 16: 4604–13.
46. Jones DT, Harris AL. (2006) Identification of novel small-molecule inhibitors of hypoxia-inducible factor-1 transactivation and DNA binding. *Mol. Cancer Ther.* 5:2193–202.
47. Gillespie DL *et al.* (2007) Silencing of hypoxia inducible factor-1alpha by RNA interference attenuates human glioma cell growth *in vivo*. *Clin. Cancer Res.* 13:2441–8.
48. Bocci G *et al.* (2004) Increased plasma vascular endothelial growth factor (VEGF) as a surrogate marker for optimal therapeutic dosing of VEGF receptor-2 monoclonal antibodies. *Cancer Res.* 64:6616–25.